ARABINOXYLAN-MEDIATED GREEN SYNTHESIS OF SILVER NANOPARTICLES WITH ENHANCED ANTIBACTERIAL AND DYE DEGRADATION EFFICIENCY

AAMNA MAJEED,[*] GULZAR MUHAMMAD,[*] MUHAMMAD RAUF RAZA,[*] MUHAMMAD AMIN,[**] AROOJ AFZAL[***] and REHANA BADAR[***]

[*]*Department of Chemistry, Government College University Lahore, 54000, Lahore, Pakistan*
[**]*Department of Chemistry, University of Lahore, Sargodha Campus, Sargodha, Pakistan*
[***]*Department of Biological Sciences, Superior University, Raiwind Road, Lahore, Pakistan*
✉ *Corresponding author: G. Muhammad, mgulzar@gcu.edu.pk*

Received March 4, 2025

This study adopted a green synthesis method to produce silver nanoparticles (Ag NPs) using arabinoxylan mucilage from *Plantago major* seeds, which naturally functions as a reducing and stabilizing agent. Different characterization techniques like UV-Vis spectroscopy, Fourier transform infrared (FTIR) spectroscopy, scanning electron microscopy (SEM), energy dispersive X-rays (EDX), and X-ray diffraction (XRD) were used to determine the morphology, composition, and surface functionality of the synthesized nanoparticles. The formation of Ag NPs was indicated by a color change from light brown to dark brown and a characteristic absorption peak at 420 nm, with increased absorption over time due to the enhanced production of NPs. FTIR analysis confirmed Ag NP formation with characteristic bands in the 400–600 cm^{-1} range. SEM analysis revealed flower-shaped Ag NPs, while XRD confirmed the face-centered cubic crystalline structure. Dynamic light scattering (DLS) analysis showed stable Ag NPs with a slightly negative surface charge (-0.1 mV). The synthesized Ag NPs exhibited effective antimicrobial activity against *Escherichia coli*, *Enterobacter aerogenes*, and *Bacillus cereus*, demonstrating superior inhibition zones, minimum inhibitory concentration (MIC), and minimum bactericidal concentration (MBC) values compared with the positive control, rifampicin. Additionally, Ag NPs demonstrated significant photocatalytic potential in water purification, degrading crystal violet (87.12%) and safranin dye (83.87%) following pseudo-first-order kinetics. The findings highlight the potential of Ag NPs as eco-friendly alternatives to synthetic wastewater treatment agents and antibiotics.

Keywords: silver nanoparticles, *Plantago major*, mucilage, dye degradation, crystal violet, safranin, antibacterial

INTRODUCTION

Polysaccharide-based mucilages from plants (seeds, leaves, and roots), *Protista* and marine algae are useful for storing food, thickening membranes, and facilitating seed germination.[1-3] The plant families rich in mucilage are *Brassicaceae*, *Plantaginaceae*, *Linaceae*, and *Acanthaceae*.[2] Polysaccharides in the mucilages mainly include pectin and hemicelluloses.[1] Plants produce biocompatible, non-toxic, and biodegradable mucilages that can serve as additives to make low-fat, prebiotic foods.[3] Mucilages swell in water with a higher water holding capacity due to the hydrophilic functional groups (-OH, NH_2, -COOH, -$CONH_2$), cross-linking, and porosity in the polymer structure. Mucilages are widely used in medicinal, environmental conservation, and commercial applications, including tissue engineering, wound healing, drug delivery,[4] wastewater treatment, cosmetics, agriculture, pharmaceuticals, horticulture, engineering, and diapers.[5] Mucilage-based polysaccharides respond to stimuli such as temperature, pH, ionic strength, and solvents,[6] enhancing their significance for sustainable drug delivery systems.[7] The literature revealed the utilization of smart mucilages from *Mimosa pudica* and flaxseed for drug delivery applications.[8]

P. major L. (plantain – broadleaf) is an herbaceous plant with oval-shaped seeds that extrude mucilage on drenching in water. Different plant parts have been found to exhibit significant antioxidant, antibacterial, immune-enhancing,

anticancer, and anti-inflammatory effects.[9] Traditionally, the plant is used to treat ocular, dermal, digestive, reproductive, ear and respiratory diseases, and is considered to have wound-healing effects.[10] The extracts from various plant parts have potential against stomach disorders (such as swelling, intestinal infection, ulcers, constipation, bleeding, hematemesis, stomach pain, and diarrhea), neurological disorders (like epilepsy), liver disorders, and uterine disorders (including tumors, ulcers, heavy uterine bleeding, and frequent menstrual disorders like polymenorrhea).[11] The plant acts as a diuretic drug and is prescribed for bladder and kidney pain, urinary infection, and hematocyturia.[12] The plant is effective against dermal infections and cures head and face lesions, and skin ulcers.[13] Biodegradable and biocompatible polysaccharide-based mucilage from *P. major* seeds comprises monosaccharides (xylose, glucose, galacturonic acid, galactose, arabinose, and glucuronic acid), disaccharides (sucrose), and a trisaccharide (planteose).[14] The mucilage was found to possess a high swelling index, viscosity, water-holding capacity, and mucoadhesive properties.[15] Mucilage extruded from seeds of *P. major* sustained the release of propranolol hydrochloride in tablet formulations.[16]

Different morphologies (nano-powder, nano-crystals, and nano-clusters) and sizes of NPs (1-100 nm) exhibited a wide range of applications.[17] Nanomaterials have been developed for new industrial trends and advancements in novel products,[18] catalysis,[19] biological sensing, drug delivery,[20] pathogen detection,[21] tissue engineering,[22] and wastewater treatment.[23] Textile and other industries discharge heavy metals[24] and dyes into water, contaminating water resources.[25] Wastewater remediation is critical because of the carcinogenic nature of dyes. Different physical, biological, and chemical methods for wastewater treatment[26] do not adequately remove dyes.[27] NPs (Cu, Au, Pd, Ag, and Fe) used as photocatalysts degrade dyes, such as methyl orange, methylene blue, and crystal violet, primarily due to their higher absorption capacity, larger surface area, and faster equilibrium rates.[28] Ag NPs, due to their eco-friendly, non-toxic, and biodegradable nature, are considered the most effective for dye degradation.

Metallic NPs exhibit catalytic activity due to their specific size and shape, and are widely used as catalysts for organic and inorganic reactions.[29] Biosynthesized metallic NPs are diversely used to remove organic pollutants and dyes[30] due to their lower cost and significant environmental remediation abilities.[31] Ag NPs also exhibited significant optical properties in visible and near-IR regions due to their nano size and shape.[32] Ag NPs exhibit greater chemical stability and are good electrical conductors, thereby enhancing their physicochemical properties for use as sensors and conductors.[33] Further applications of Ag NPs include the degradation of organic, inorganic, aromatic, and carcinogenic dyes for wastewater treatment, as well as their use as antibacterial agents.[34]

In this work, we synthesized Ag NPs using *P. major* seed mucilage, which serves as both reducing and stabilizing agent. The synthesized NPs were characterized using scanning electron microscopy (SEM) for morphology, X-ray diffraction (XRD) for structure determination, energy-dispersive X-ray spectroscopy (EDX) for elemental composition, UV-visible spectroscopy for absorption, and Fourier-transform infrared spectroscopy (FTIR) for surface interaction. The antimicrobial activity of the Ag NPs was evaluated against Gram-positive and Gram-negative bacterial strains (*E. coli*, *E. aerogenes*, and *B. cereus*) by measuring the zone of inhibition (ZOI), minimal inhibitory concentration (MIC), and minimum bactericidal concentration (MBC). Moreover, the prepared Ag NPs were used for photocatalytic dye degradation.

EXPERIMENTAL

Materials

Silver nitrate ($AgNO_3$) was purchased from Merck, Germany, and *P. major* seeds were purchased from a local market. *B. licheniformis*, *E. coli*, and *Aeromonas* strains were obtained from the Microbiology Laboratory in the Department of Zoology, Government College University, Lahore. Highly pure chemicals or reagents were used for this study.

Mucilage extraction

After cleaning the seeds, mucilage was extracted using deionized water using the hot-water extraction method. In this method, water is preheated to a specific temperature, seeds are added, and the mixture is heated until the mucilage is extracted. The extracted mucilage is separated from the seeds by muslin cloth, spread on Petri dishes, and dried in an oven at 80 °C for further use.

Ag NPs synthesis

The silver nitrate solution (1.0 mM, 10 mL) and the mucilage suspension (1.0%, 10 mL) were prepared separately and mixed before exposure to sunlight to observe the color change (Fig. 1). A dark brown color was obtained, indicating the formation of Ag NPs. The

color intensity changed over time as more silver ions were reduced and stabilized to Ag NPs. Ag NPs were centrifuged and analyzed by UV-visible spectrophotometry.

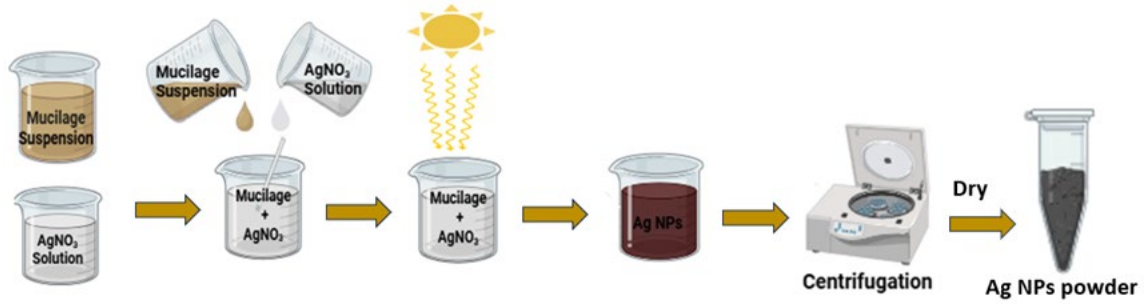

Figure 1: Schematic illustration showing the synthesis of Ag NPs from mucilage and $AgNO_3$

Characterization of Ag NPs

Different spectroscopic techniques, UV-visible spectroscopy (Agilent Cary 60), with a wavelength range of 800-200 nm, and FTIR spectroscopy, using an FTIR spectrophotometer (Agilent Cary 630) in the wavenumber range of 4000–400 cm^{-1}, were used to characterize and investigate the possible functional groups involved in the surface modification and stabilization of Ag NPs. SEM (Nova Nano SEM 450) and XRD were used to determine the morphology and crystalline structure of Ag NPs. SEM equipped with EDX at 10 kV was used for elemental analysis, and XRD was performed by placing the thin sample layer on a glass substrate using the Proto AXRD LPD X-ray diffractometer. The stability and size distribution of Ag NPs were further investigated by DLS and Zeta potential measurements using a Litesizer 500 (Omega cuvette, Mat. No. 225288).

Antibacterial activity

The antibacterial activity of synthesized Ag NPs was analyzed against three bacterial strains (*E. coli*, *E. aerogenes* and *B. cereus*) using the Agar well diffusion method. Initially, pathogen strains were prepared, with the turbidity standard concentration adjusted to 0.5 McFarland. Five Mueller-Hinton agar plates were prepared, and the strains were spread on them using sterile cotton buds. Ag NPs at concentrations of 100, 50, and 25 µg/mL were added to the wells, except for the control. The rifampicin (50 µg mL^{-1}) served as a positive control, while a mixture of ethanol and water (1:1) was used as a negative control. Each experiment was performed three times to ensure accuracy in results.

Determination of MIC and MBC

MICs of synthesized Ag NPs against the strains were measured using 24-hour-old cultures. Nutrient broth (3.0 mL) was prepared and added to a sterile test tube before mixing the bacterial culture (30 µL) for each sample. The serial concentrations of Ag NPs (5-30 µg mL^{-1}) were mixed in all test tubes, except the negative control. Test tubes were incubated for 24 h at 37 °C. UV-Vis was used to measure the optical density at 523 nm. The samples for determining MICs were incubated at 37 °C for 24 h, and MBCs were determined by spreading them (100 µL) on nutrient agar plates.

Photocatalytic activity of Ag NPs

The photocatalytic efficiency of Ag NPs was analyzed using crystal violet and safranin dyes (50 mL, diluted to 10 ppm from initial concentrations of 5-10 mg/100 mL, with reaction times ranging from 0 to 150 minutes). Dye samples were stirred after adding NPs, then exposed to sunlight with a high UV index (10+) as per the EPA global solar index for photocatalytic degradation. The samples were taken from the mixture at regular intervals to determine the maximum absorption using a UV-visible spectrophotometer. The baseline obtained with a dye solution without NPs was compared to determine the maximum degradation efficiency under optimized conditions. The percentage degradation was calculated according to the equation given below:

$$\%\ Dye\ degradtion = \frac{C_0 - C_t}{C_t} \quad (1)$$

where C_0 is the initial concentration of the dye before adding NPs, and C_t is the final dye concentration after being treated with NPs. Dye degradation kinetics were assessed by following the equation:[35]

$$In\ \frac{C_t}{C_0} = -Kt \quad (2)$$

RESULTS AND DISCUSSION

Synthesis of Ag NPs

Arabinoxylan-based mucilage extracted from *P. major* was mixed with silver nitrate solution before exposure to sunlight. The hydroxyl groups of mucilage reduced the silver ions to silver atoms, which were further coated by the mucilage. The color of the reaction mixture changed to dark brown over time (10-50 min), confirming the successful synthesis of Ag NPs (Fig. 2).

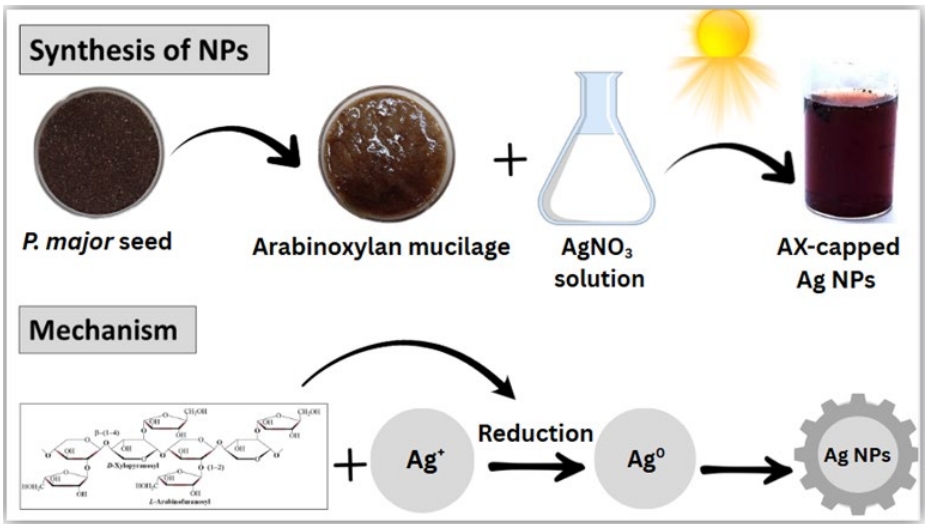

Figure 2: Reduction and stabilization of Ag NPs by the arabinoxylan (AX)-based mucilage from *P. major*

UV–visible spectra of Ag NPs

UV-Vis spectrophotometry helps identify, characterize, and study NPs because metallic NPs possess free electrons that can absorb radiation through surface plasmon resonance. The electrons of NPs exhibit vibrations that cause the resonance of electrons with electromagnetic radiations of a specific frequency. The NPs exhibited absorption in the visible range (380-450 nm). In the present work, Ag NPs showed a maximum absorption at 420 nm (Fig. 3 a), which is consistent with values reported in the literature. The absorption bands in the UV-visible spectra showed that absorption intensity increases over time (Fig. 3b). The color of Ag NPs changed to reddish brown (Fig. 3c) in about 50 minutes, supporting the increase in absorption intensity over time (Fig. 3b). The UV-visible absorption spectrum of Ag NPs after one year exhibited a peak in the same region at 420 nm (Fig. 3d), which demonstrates the stability of Ag NPs even after a year of their synthesis. The literature reported similar color changes during the formation of Ag NPs from the marine alga *Ecklonia cava*, and absorption peaks around 420-250 nm for *Punica granatum* peel.[36]

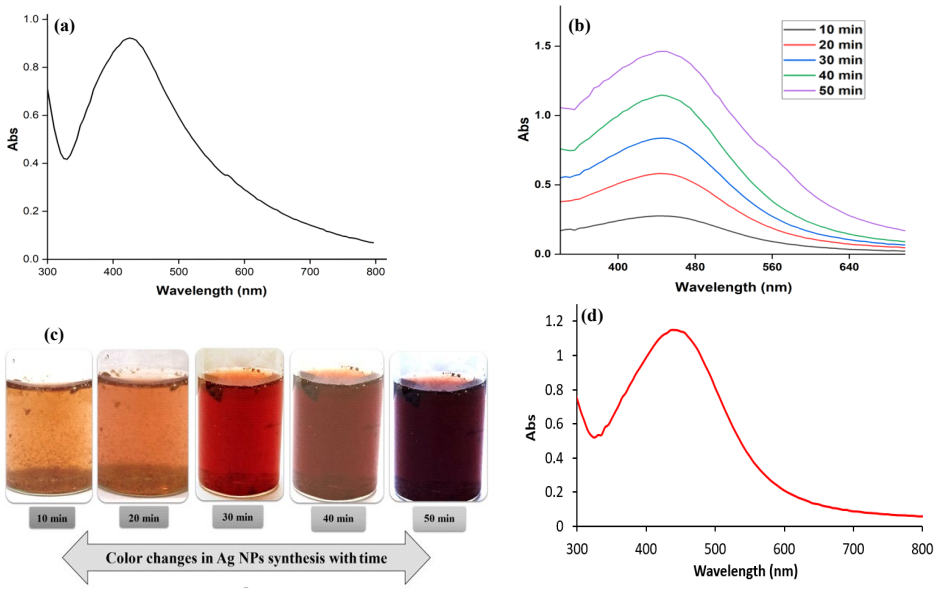

Figure 3: (a) UV-visible absorption spectrum of Ag NPs synthesized from *P. major* mucilage, (b) changes in absorption maxima over time, (c) color changes over time, (d) UV-visible absorption spectrum of Ag NPs after 1 year

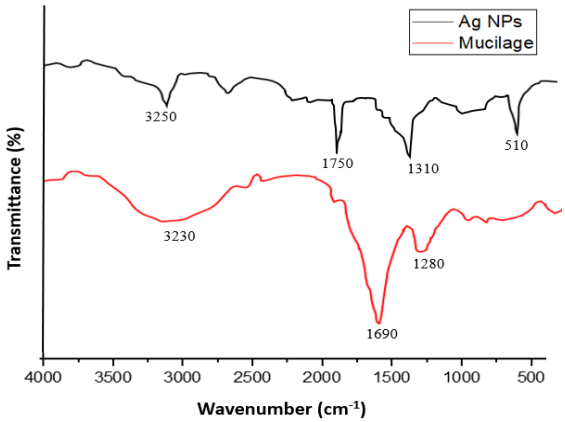

Figure 4: FTIR spectra of mucilage and Ag NPs synthesized using mucilage from *P. major* seeds

FTIR analysis of Ag NPs

FTIR spectroscopy is commonly used to assess the possible surface interaction between synthesized NPs and other molecules involved in the stabilization of NPs. FTIR analysis explains functional groups and bond types by particular wave numbers. The broad peaks for stretching vibration of O-H bonds appeared both for mucilage and Ag NPs from 3250 cm^{-1} to 3350 cm^{-1}, indicating the presence of sugars and phenolic groups in mucilage, and the peaks at 1690 cm^{-1} to 1750 cm^{-1} revealed carbonyl group (C=O) vibrations. The stretching vibrations at 1250 cm^{-1} and 1306 cm^{-1} are possibly due to C-O bonds.[37] The stretching vibration at 580 cm^{-1} resembles the Ag-O bonds in the Ag NPs spectrum (Fig. 4).[38]

The mucilage peaks slightly differ from those in the Ag NPs spectrum. A significant difference between simple mucilage and synthesized NPs lies in the presence of Ag-O bonds (580 cm^{-1}), which confirms the formation of Ag NPs. Although other peaks appeared in a similar spectrum range, the peaks of NPs slightly shifted to higher values, indicating the interaction of functional groups present in the mucilage on the surface of NPs. This shift in NPs peaks demonstrates the significant binding and stabilization of NPs by the mucilage.[39]

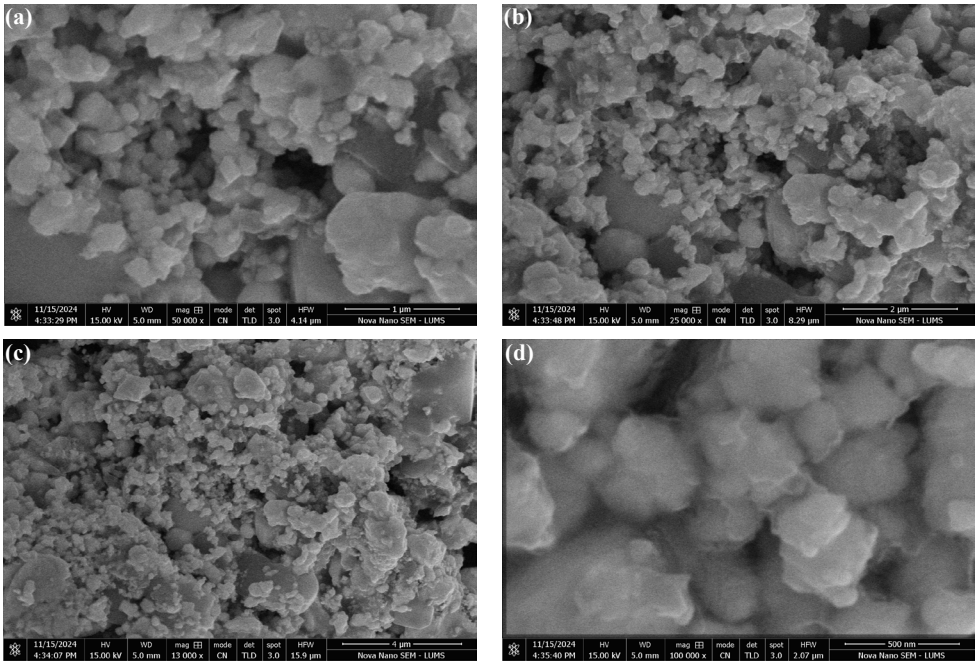

Figure 5: SEM images of Ag NPs scanned at scales of 1 µm (a), 2 µm (b), 4 µm (c), and 500 nm (d)

SEM analysis

Literature discovered typical circular, cubical, triangular, elliptical, and pebble-like shapes of Ag NPs.[40] In this study, SEM analysis of Ag NPs showed a flower-shaped morphology at magnifications of 1 µm, 2 µm, 4 µm, and 500 nm (Fig. 5), with an average size of 110 nm. Ag NPs from sapota fruit waste exhibited a spherical shape (30 nm).[41] Similarly, Ag NPs were synthesized from purified apiin compound, extracted from henna leaf,[42] green tea, and *C. sinensis* extract.[43] The Ag NPs are not uniformly distributed because the shape and size of the NPs depend upon interactions of the NPs with functional groups in the biomolecules.

DLS analysis

The particle size distribution and charge of the Ag NPs were measured using DLS. There are three distinct peaks in the spectrum, representing the particle-size distribution of Ag NPs (Fig. 6a). The most prominent peak covers 64.62% of the Ag NPs and has an average particle size of 132.27 nm. In contrast, the second major peak covers 34.32% of the total area of the nanoparticles, with an average size of 1125.3 nm, and the larger NPs are due to Ag NP aggregation. The smallest peak covers only 1% of the area, with an average particle size of 5.62 nm. The polydispersity index (PDI) value of 0.27 confirms that the particles are not uniform, and the presence of different peaks in the spectrum confirms a mixture of different particle sizes of the Ag NPs.

Further, the stability of the Ag NPs was assessed by zeta potential. The surface charge, whether positive or negative, significantly controls nanoparticle aggregation. The increase in charge density reduces particle size. In contrast, zeta potential distribution for Ag NPs (Fig. 6b) exhibits a sharp peak at −0.1 mV, showing that Ag NPs have a slightly negative surface and are stabilized by the steric hindrance of mucilage molecules adsorbed on the surface of Ag NPs.[44] Studies reporting similar size distributions from DLS analysis of *P. major* seed extract in the literature confirmed the synthesis and stability of Ag NPs synthesized in our study from seed mucilage.[45]

EDX analysis

EDX analysis was used for compositional and elemental analysis of NPs. The EDX spectrum of Ag NPs synthesized from PM mucilage shows a significant peak of Ag (80.59%), along with O, C, Ca, Si, and Na peaks (Fig. 7). The EDX spectrum also showed elements such as carbon and oxygen, owing to the polysaccharide nature of the mucilage, which contains arabinoxylans, flavonoids, and phenolic compounds.

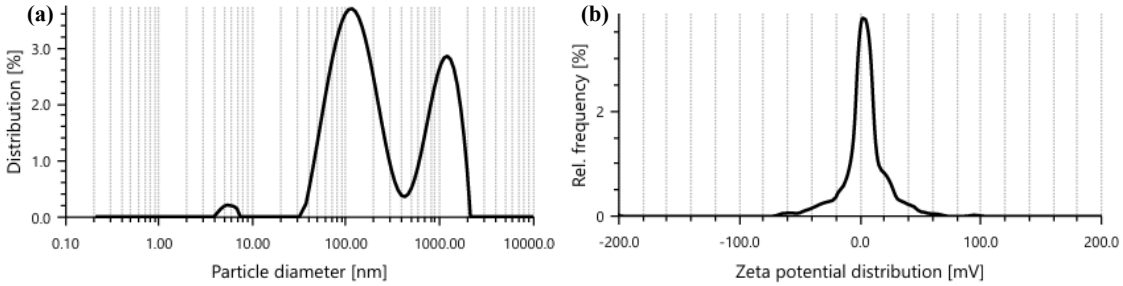

Figure 6: Particle size distribution (a) and Zeta potential distribution (b) of Ag NPs

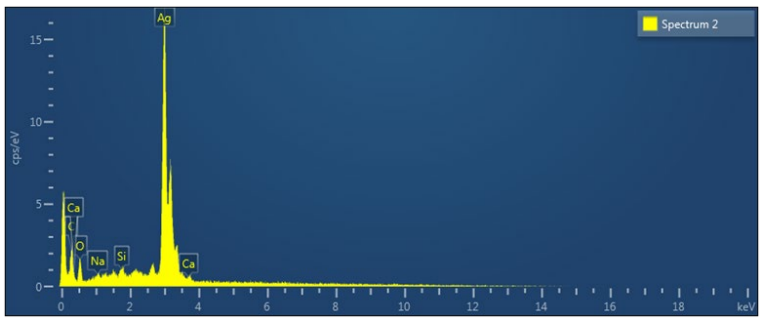

Figure 7: EDX spectrum of Ag NPs showing silver as the main element

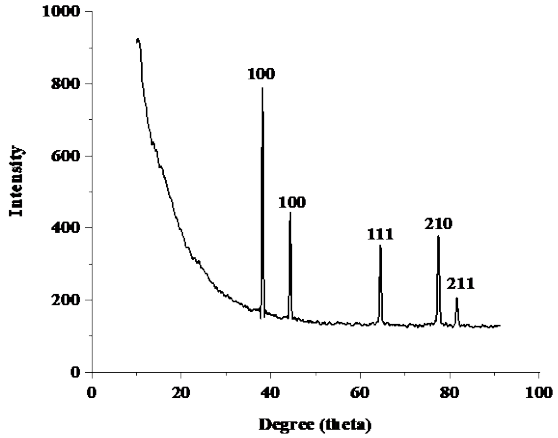

Figure 8: XRD spectrum of Ag NPs showing their crystalline nature

Elements, such as Ca, Na, and Si, may be due to impurities or to the apparatus used to prepare and analyze samples. EDX analysis of Ag NPs synthesized using flaxseed mucilage presented similar elements, namely, carbon, oxygen, calcium, potassium, and magnesium due to polysaccharides, sugars, and minerals present in the mucilage.[46]

X-ray diffraction analysis

The XRD spectrum of Ag NPs (Fig. 8) depicted 2θ angles of 38.34°, 44.55°, 64.55°, 77.54°, and 81.60° corresponding to the crystalline planes (100), (100), (111), (210), and (211). The faces established the face-centered cubic structure of Ag NPs, which is the same pattern as that synthesized from the extract of P. *lanceolate*.[47] Moreover, high-intensity peaks in the XRD spectrum revealed the crystalline structure of Ag NPs from the marine alga *Ecklonia cava*, as confirmed by the planes observed in the XRD pattern.[48]

Antimicrobial activity

Ag NPs attached to the cell wall and cytoplasmic membrane through electrovalent attractions, inhibited the growth of microorganisms.[49] Moreover, Ag ions also showed strong attraction to sulfur proteins. The channel proteins, cation-selective porins, provide a possible pathway for Ag ions to enter the cell. The exposure of cells to Ag NPs generates intracellular reactive oxygen species (ROS), which inhibit respiratory enzymes and disrupt membranes and DNA.[50] The antimicrobial activity of Ag NPs was analyzed against three pathogen strains, such as *E. coli*, *E. aerogenes* and *B. cereus* (Fig. 9a-c).

Ag NPs inhibited the growth of *E. coli* (ZOI 24±0.55 mm) more effectively, followed by *B. cereus* (ZOI 21±0.66 mm) and *E. aerogenes* (ZOI 17±0.66 mm) (Fig. 9d). Ag NPs showed greater potential against Gram-negative bacteria than Gram-positive bacteria.

Previous studies showed that Ag NPs derived from *Citrus limon* zest inhibit bacterial growth, with a zone of inhibition ranging from 8 to 20 mm.[56] The obtained MICs and MBCs against the three pathogen strains are shown in Figure 9e. The MIC values were 10, 15, and 5 μgmL^{-1} for *E. coli*, *B. cereus*, and *E. aerogenes*, respectively, while the MBC values were 15, 15, and 10 μgmL^{-1} for the same species. MIC and MBC results showed that green-synthesized Ag NPs provided greater inhibition zones against the pathogenic bacteria tested in this study at low concentrations.

Photocatalytic activity of Ag NPs

The crystallographic structure, shape, and size of nanoparticles determine the photocatalytic activity. The photocatalytic activity against crystal violet and safranin dyes was assessed using Ag NPs via UV-Vis analysis. The color disappearance of dye solutions indicated the degradation of dyes. Ag NPs demonstrated significant degradation (Fig. 11a, b, c) of crystal violet (87.12%) and safranin (83.87%), with optimum NPs dosage (5 mg), dye concentration (50 mL, 10 ppm diluted from 5.0 mg/100 mL), and sunlight exposure (150 min).

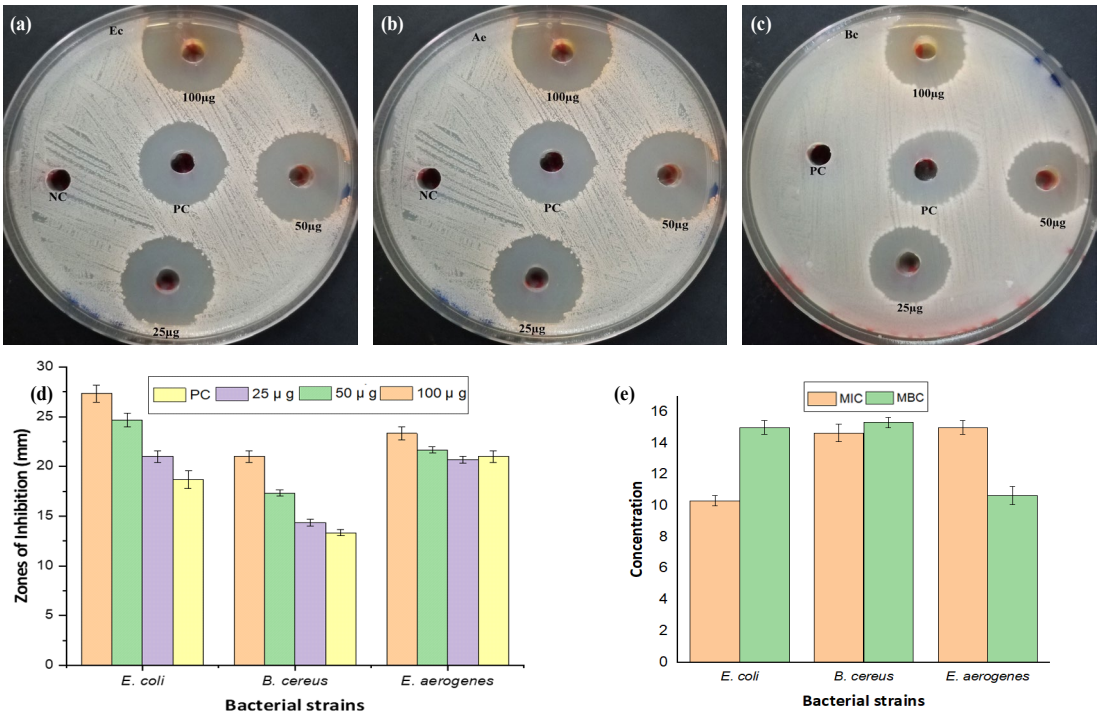

Figure 9: Antimicrobial potential of Ag NPs against three pathogen strains, *E. coli* (a), *E. aerogenes* (b), and *B. cereus* (c), zones of inhibition against different bacteria (d), and MIC and MBC values (e)

Table 1
Antimicrobial potential comparison of Ag NPs synthesized from different sources using a green approach

Extract/species used	Pathogen	Method	ZOI (mm)	Ref.
Radish microgreen	*S. aureus* *E. coli*	Well diffusion (Agar) method	15 15	51
C. roxburghii	*E. coli* *P. aeruginosa* *M. luteus* *B. subtilis* *E. aerogenes* *S. aureus*	Well diffusion (Agar) method	16 21 19 17 18 12	52
Fenugreek	*S. aureus* *E. coli*	Agar well diffusion method	9 10	53
Streptomyces sp.	*S. aureus* *E. faecalis* *K. pneumonia* *E. coli*	Disc diffusion method	22 15 19 17	54
Chlorella vulgaris	*E. coli* *P. aeruginosa*	Agar well diffusion method	20 21	55
P. major mucilage	*E. coli* *E. aerogenes* *B. cereus*	Agar well diffusion method	24 17 21	Present study

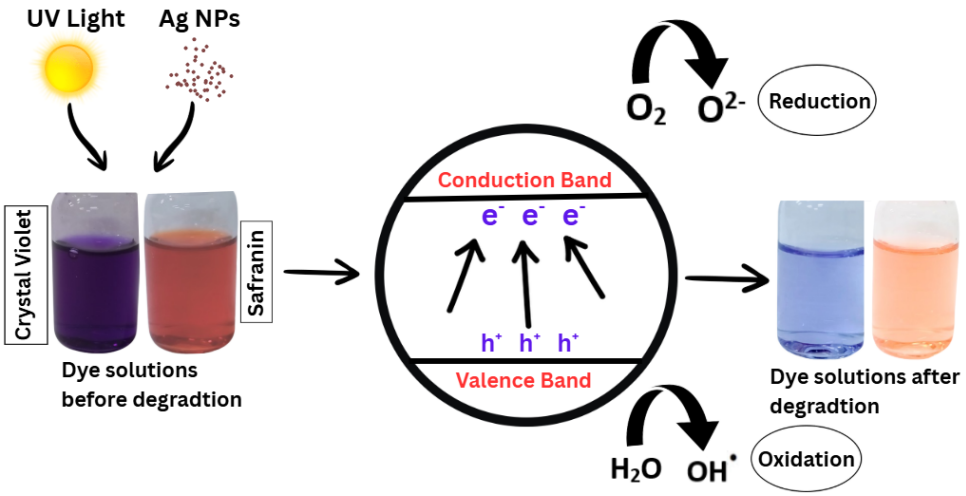

Figure 10: Degradation mechanism of dye solutions by Ag NPs on exposure to sunlight

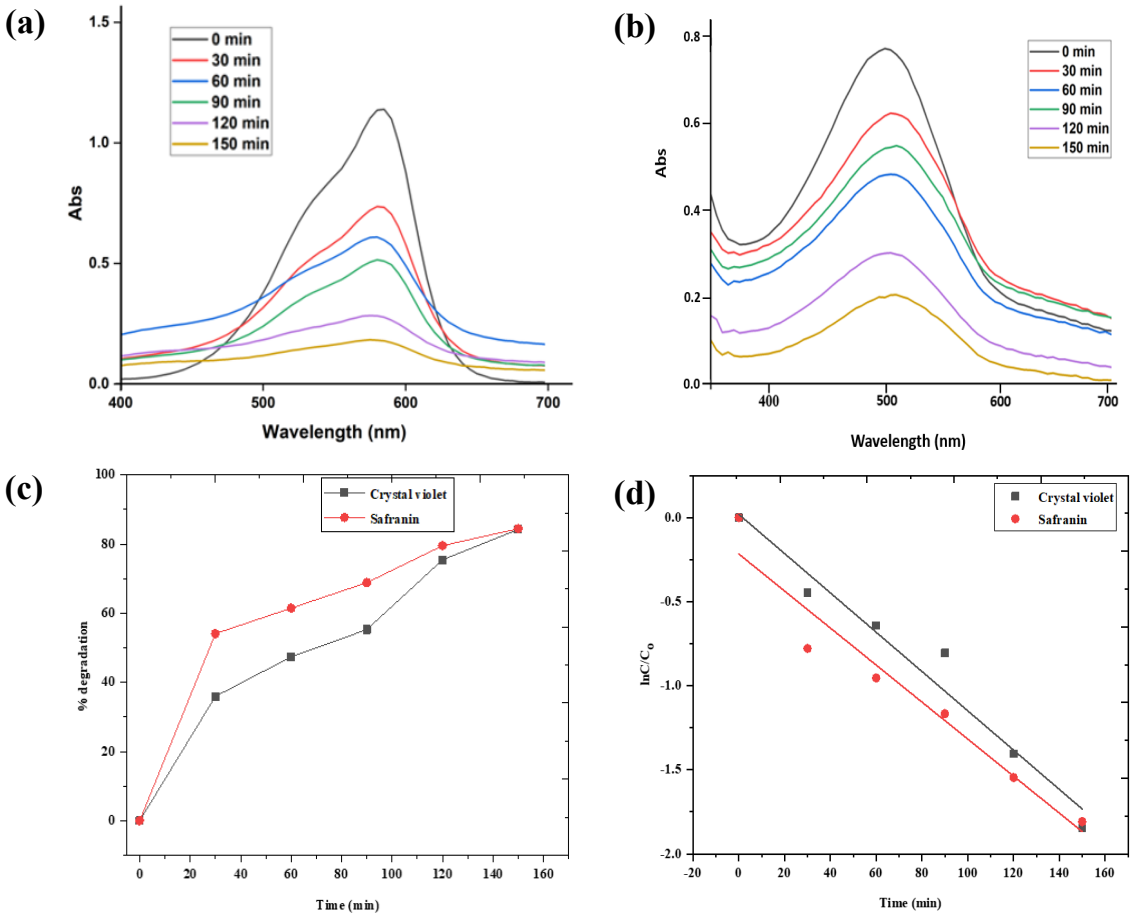

Figure 11: Degradation of (a) crystal violet and (b) safranin by Ag NPs in sunlight; degradation of crystal violet and safranin over time (c), and degradation kinetics (d)

Table 2
Dye degradation potential of Ag NPs reported in previous literature

Plant	Part	Time	Light source	Pollutant	Degradation, %	Ref.
Ruellia tuberosa	Leaves	180 min	Sunlight	Crystal violet	87%	60
Radish Microgreen	Plant	14 min	Sunlight	Crystal violet	96.90%	61
Carissa carandas	Fruit	150 min	Sunlight	Crystal violet	93%	62
		180 min	Sunlight	Crystal violet	90%	63

Sanguisorba officinalis	Leaves and stem			Safranin	90%	
Saussurea costus	Root	72 h	In dark	Safranin	84.6%	64
P. major mucilage	Seeds	150 min	Sunlight	Crystal violet Safranin	87.12% 83.87%	Present study

Crystal violet undergoes greater degradation in the presence of NPs due to its triphenylmethane structure, which contains more delocalized π-electrons from aromatic rings.[57] These electrons enhance the binding of the dye to the surface of NPs through rapid electron transfer, leading to greater dye removal from wastewater and higher degradation percentages than safranin, which has a less aromatic structure and exhibits a lower rate.[58] The mechanism of dye degradation involves the creation of an electron-hole pair when electrons are excited from the valence to the conduction band, leading to the formation of free radicals that degrade the dye.[59]

Furthermore, to determine degradation kinetics, the Langmuir-Hinshelwood model was used. According to this model, the dye-degradation reactions of crystal violet and safranin follow pseudo-first-order kinetics ($R^2 > 0.9$) (Fig. 11d). From the experiment, the rate constant K for crystal violet is 0.012/min, and for safranin, it is 0.011/min.

CONCLUSION

Ag NPs were synthesized by a green synthesis method from PM mucilage. The findings of the study, namely UV-visible spectroscopy (λ_{max} = 420 nm), with the time graphs illustrating color changes from light to dark brown, FTIR analysis ($\bar{\upsilon}$ = 520, 1300, and 3392 cm^{-1}), and SEM observation (average diameter 110 nm), confirmed the synthesis of Ag NPs. Elemental analysis by EDX revealed the predominant presence of Ag (80.59%) with trace amounts of other elements, and XRD showed an FCC structure. DLS indicated stable Ag NPs with a slightly negative surface. Reaction progress was analyzed by observing color changes. The synthesized Ag NPs exhibited significant antimicrobial activity against *B. licheniformis*, *E. coli*, and *Aeromonas* sp.

Furthermore, Ag NPs synthesized via this green route from arabinoxylan mucilage were used efficiently as eco-friendly photocatalysts for the degradation of crystal violet and safranin solutions. The process followed pseudo-first-order kinetics. Ag NPs demonstrated good antioxidant potential and were effective for dye degradation. Furthermore, Ag NPs have the advantages of being small, stable, and having effective catalytic and antibacterial activities. The reaction can be controlled and experimental data can be reproduced by maintaining similar reaction conditions (silver nitrate and mucilage concentration, exposure time, and a fixed time of day with similar light intensity), resulting in consistent results.

REFERENCES

[1] B. E. Campos, T. D. Ruivo, M. R. da Silva Scapim, G. S. Madrona and R. D. C. Bergamasco, *LWT*, **65**, 874 (2016), https://doi.org/10.1016/j.lwt.2015.09.021

[2] R. Waghmare, J. A. Moses and C. Anandharamakrishnan, *Crit. Rev. Food Sci. Nutr.*, **62**, 4186 (2022), https://doi.org/10.1080/10408398.2021.1873730

[3] M. Cai, N. Wang, C. Xing, F. Wang, K. Wu *et al.*, *Environ. Sci. Pollut. Res.*, **20**, 8924 (2013), https://doi.org/10.1007/s11356-013-1815-6

[4] I. F. da Silveira Ramos, L. M. Magalhães, C. do O. Pessoa, P. M. P. Ferreira, M. dos Santos Rizzo *et al.*, *Ind. Crop. Prod.*, **171**, 113981 (2021), https://doi.org/10.1016/j.indcrop.2021.113981

[5] R. Singh and D. Barreca, in "Recent Advances in Natural Products Analysis", edited by A. Sanches Silva, S. F. Nabavi, M. Saeedi and S. M. Nabavi, Elsevier, 2020, p. 663, https://doi.org/10.1016/B978-0-12-816455-6.00021-4

[6] R. Po, *J. Macromol. Sci., Part C: Polym. Rev.*, **34**, 607 (1994), https://doi.org/10.1080/15321799408014168

[7] A. Ali, M. A. Hussain, A. Abbas, T. A. Khan, G. Muhammad *et al.*, *Cellulose Chem. Technol.*, **56**, 239 (2022), https://doi.org/10.35812/CelluloseChemTechnol.2022.56.22

[8] D. Z. Liu, M. T. Sheu, C. H. Chen, Y. R. Yang and H. O. Ho, *J. Control. Release*, **118**, 333 (2007), https://doi.org/10.1016/j.jconrel.2007.01.001

[9] M. T. Haseeb, M. A. Hussain, S. H. Yuk, S. Bashir and M. Nauman, *Carbohyd. Polym.*, **136**, 750 (2016), https://doi.org/10.1016/j.carbpol.2015.09.092

[10] B. M. Abd Razik, H. A. Hasan and M. K. Murtadha, *Iraq. Postgrad. Med. J.*, **11**, 130 (2012), https://doi.org/10.1016/j.jtcme.2017.09.002

[11] L. C. Chiang, W. Chiang, M. Y. Chang, L. T. Ng and C. C. Lin, *Antiviral Res.*, **55**, 53 (2002), https://doi.org/10.1016/S0166-3542(02)00007-4

[12] E. Akhtari, H. Tajadini and M. Khazanehha, *Tradit. Integr. Med.*, **22**, 218 (2018), https://doi.org/10.2174/2215083806666191202145837

[13] A. R. Derakhshan, *J. Evid.-Based Complement. Altern. Med.*, **22**, 324 (2017), https://doi.org/10.1177/2156587216650302
[14] B. Javadi, A. Sahebkar and S. A. Emami, *Iran. J. Basic Med. Sci.*, **16**, 1 (2013)
[15] N. S. Karamova, D. G. Fatykhova, Y. R. Abdrakhimova and O. N. Il'inskaya, *Russ. J. Genet.: Appl. Res.*, **1**, 371 (2011), https://doi.org/10.1134/S207905971105008X
[16] A. B. Samuelsen, *J. Ethnopharmacol.*, **71**, 1 (2000), https://doi.org/10.1016/S0378-8741(00)00212-9
[17] M. Saeedi, K. Morteza-Semnani and M. Sagheb-Doust, *Acta Pharm.*, **63**, 99 (2013), https://doi.org/10.2478/acph-2013-0010
[18] C. R. Rao, G. U. Kulkarni, P. J. Thomas and P. P. Edwards, *Chem. Soc. Rev.*, **29**, 27 (2000), https://doi.org/10.1039/A904518J
[19] W. J. Stark, P. R. Stoessel, W. Wohlleben and A. J. Hafner, *Chem. Soc. Rev.*, **44**, 5793 (2015), https://doi.org/10.1039/C4CS00362D
[20] D. L. Fedlheim and C. A. Foss, "Metal Nanoparticles: Synthesis, Characterization, and Applications", CRC Press, 2001, https://doi.org/10.1201/9780367800475
[21] M. De, P. S. Ghosh and V. M. Rotello, *Adv. Mater.*, **20**, 4225 (2008), https://doi.org/10.1002/adma.200703183
[22] R. L. Edelstein, C. R. Tamanaha, P. E. Sheehan, M. M. Miller, D. R. Baselt *et al.*, *Biosens. Bioelectron.*, **14**, 805 (2000), https://doi.org/10.1016/S0956-5663(99)00054-8
[23] A. De La Isla, W. Brostow, B. Bujard, M. Estevez, J. R. Rodriguez *et al.*, *Mater. Res. Innov.*, **7**, 110 (2003), https://doi.org/10.1080/14328917.2003.11784770
[24] T. Esakkimuthu, D. Sivakumar and S. Akila, *Pollut. Res.*, **33**, 567 (2014)
[25] Z. Fatima, A. Azam, M. Z. Iqbal, R. Badar and G. Muhammad, *Desalin. Water Treat.*, **319**, 100553 (2024), https://doi.org/10.1016/j.dwt.2024.100553
[26] P. Xu, G. M. Zeng, D. L. Huang, C. L. Feng, S. Hu *et al.*, *Sci. Total Environ.*, **424**, 1 (2012), https://doi.org/10.1016/j.scitotenv.2012.02.023
[27] V. K. Gupta, R. Jain, A. Mittal, T. A. Saleh, A. Nayak *et al.*, *Mater. Sci. Eng.* C, **32**, 12 (2012), https://doi.org/10.1016/j.msec.2011.08.018
[28] A. Miri, H. O. Shahraki Vahed and M. Sarani, *Res. Chem. Intermed.*, **44**, 6907 (2018), https://doi.org/10.1007/s11164-018-3529-3
[29] Q. Li, S. Mahendra, D. Y. Lyon, L. Brunet, M. V. Liga *et al.*, *Water Res.*, **42**, 4591 (2008), https://doi.org/10.1016/j.watres.2008.08.015
[30] N. Gupta, H. P. Singh and R. K. Sharma, *J. Mol. Catal. A: Chem.*, **335**, 248 (2011), https://doi.org/10.1016/j.molcata.2010.12.001
[31] S. Javed, M. R. Raza, M. U. Sharif, A. Majeed, M. A. Hussain *et al.*, *Desalin. Water Treat.*, **318**, 100388 (2024), https://doi.org/10.1016/j.dwt.2024.100388
[32] V. Seerangaraj, S. Sathiyavimal, S. N. Shankar, J. G. T. Nandagopal, P. Balashanmugam *et al.*, *J. Environ. Chem. Eng.*, **9**, 105088 (2021), https://doi.org/10.1016/j.jece.2021.105088
[33] L. Rastogi and J. Arunachalam, *Mater. Chem. Phys.*, **129**, 558 (2011), https://doi.org/10.1016/j.matchemphys.2011.04.068
[34] M. R. Bindhu and M. Umadevi, *Spectrochim. Acta A: Mol. Biomol.*, **135**, 373 (2015), https://doi.org/10.1016/j.saa.2014.07.045
[35] A. Ahmad, Y. Wei, F. Syed, K. Tahir, A. U. Rehman *et al.*, *Microb. Pathog.*, **102**, 133 (2017), https://doi.org/10.1016/j.micpath.2016.11.030
[36] G. Muhammad, K. N. Laila, M. U. Sharif, M. A. Hussain, A. Majeed *et al.*, *Cellulose Chem. Technol.*, **58**, 637 (2024), https://doi.org/10.35812/CelluloseChemTechnol.2024.58.58
[37] T. J. I. Edison and M. Sethuraman, *Spectrochim. Acta A Mol. Biomol. Spectrosc.*, **104**, 262 (2013), https://doi.org/10.1016/j.saa.2012.11.084
[38] H. Agarwal, K. S. Venkat and S. Rajeshkumar, *J. Microbiol. Biotechnol. Food Sci.*, **7**, 371 (2018), https://doi.org/10.15414/jmbfs.2018.7.4.371-376
[39] M. P. Naghshbandi and H. Moghimi, *Method. Enzymol.*, **630**, 431 (2020), https://doi.org/10.1016/bs.mie.2019.10.013
[40] M. G. Garnica-Romo, V. Coria-Caballero, E. Tranquilino-Rodríguez, N. Dasgupta-Schubert, M. Villicaña-Méndez *et al.*, *J. Inorg. Organomet. Polym. Mater.*, **31**, 3406 (2021), https://doi.org/10.1007/s10904-021-01968-5
[41] S. Tang, X. Meng, H. Lu and S. Zhu, *Mater. Chem. Phys.*, **116**, 464 (2009), https://doi.org/10.1016/j.matchemphys.2009.04.004
[42] C. Vishwasrao, B. Momin and L. Ananthanarayan, *Waste Biomass Valoriz.*, **10**, 2353 (2019), https://doi.org/10.1007/s12649-018-0230-0
[43] J. Kasthuri, S. Veerapandian and N. Rajendiran, *Colloids Surf. B Biointerfaces*, **68**, 55 (2009), https://doi.org/10.1016/j.colsurfb.2008.09.021
[44] A. R. Vilchis-Nestor, V. Sánchez-Mendieta, M. A. Camacho-López, R. M. Gómez-Espinosa, M. A. Camacho-López *et al.*, *Mater. Lett.*, **62**, 3103 (2008), https://doi.org/10.1016/j.matlet.2008.01.138
[45] A. K. Alzubaidi, W. J. Al-Kaabi, A. A. Ali, S. Albukhaty, H. Al-Karagoly *et al.*, *Appl. Sci.*, **13**, 2182 (2023), https://doi.org/10.3390/app13042182
[46] G. Nikaeen, S. Yousefinejad, S. Rahmdel, F. Samari and S. Mahdavinia, *Sci. Rep.*, **10**, 9642 (2020), https://doi.org/10.1038/s41598-020-66357-3
[47] M. G. Garnica-Romo, V. Coria-Caballero, E. Tranquilino-Rodríguez, N. Dasgupta-Schubert, M. Villicaña-Méndez *et al.*, *J. Inorg. Organomet. Polym. Mater.*, **31**, 3406 (2021), https://doi.org/10.1007/s10904-021-01968-5
[48] M. Z. Shah, Z.-H. Guan, A. U. Din, A. Ali, A. U. Rehman *et al.*, *Sci. Rep.*, **11**, 20754 (2021), https://doi.org/10.1038/s41598-021-00296-5
[49] J. Venkatesan, S. K. Kim and M. S. Shim, *Nanomaterials*, **6**, 235 (2016),

https://doi.org/10.3390/nano6120235
[50] M. A. Hussain, A. Shaheen, S. Z. Hussain, I. Hussain, M. T. Haseeb *et al*., *Cellulose Chem. Technol*., **57**, 993 (2023), https://doi.org/10.35812/CelluloseChemTechnol.2023.57.87
[51] J. S. McQuillan and A. M. Shaw, *Nanotoxicology*, **8**, 177 (2014), https://doi.org/10.3109/17435390.2013.870243
[52] Y. Khane, K. Benouis, S. Albukhaty, G. M. Sulaiman, M. M. Abomughaid *et al*., *Nanomaterials*, **12**, 2013 (2022), https://doi.org/10.3390/nano12122013
[53] M. A. Ashkar, A. Babu, R. Joseph, S. K. Rani and N. Vasimalai, *Inorg. Chem. Commun*., **156**, 111225 (2023), https://doi.org/10.1016/j.inoche.2023.111225
[54] P. Balashanmugam and P. T. Kalaichelvan, *Int. J. Nanomed*., **10**, 87 (2015), https://doi.org/10.2147/IJN.S79984
[55] B. Senthil, T. Devasena, B. Prakash and A. Rajasekar, *J. Photochem. Photobiol. B Biol*., **177**, 1 (2017), https://doi.org/10.1016/j.jphotobiol.2017.10.010
[56] G. B. Sheik, A. I. Raheim, Z. A. Alzeyadi and M. I. AlGhonaim, *Asian J. Biol. Life Sci*., **8**, 89 (2019), https://doi.org/10.5530/ajbls.2019.8.15
[57] J. Annamalai and T. Nallamuthu, *Appl. Nanosci*., **6**, 259 (2016), https://doi.org/10.1007/s13204-015-0426-6
[58] D. F. Duxbury, *Dyes Pigment*., **25**, 179 (1994), https://doi.org/10.1016/0143-7208(94)85044-5
[59] S. Göktürk and M. Tunçay, *Spectrochim. Acta A Mol. Biomol. Spectrosc*., **59**, 1857 (2003), https://doi.org/10.1016/S1386-1425(02)00418-3
[60] S. Marimuthu, A. J. Antonisamy, S. Malayandi, K. Rajendran, P. C. Tsai *et al*., *J. Photochem. Photobiol. B*, **205**, 111823 (2020), https://doi.org/10.1016/j.jphotobiol.2020.111823
[61] V. Seerangaraj, S. Sathiyavimal, S. N. Shankar, J. G. T. Nandagopal, P. Balashanmugam *et al*., *J. Environ. Chem. Eng*., **9**, 105088 (2021), https://doi.org/10.1016/j.jece.2021.105088
[62] M. A. Ashkar, R. Arjun Babu, R. Joseph, S. K. Rani and N. Vasimalai, *Inorg. Chem. Commun*., **156**, 111225 (2023), https://doi.org/10.1016/j.inoche.2023.111225
[63] N. Anupama and G. Madhumitha, *Inorg. Nano-Met. Chem*., **47**, 116 (2017), https://doi.org/10.1080/15533174.2016.1149731
[64] S. Baker, O. V. Perianova, S. V. Prudnikova, A. Kuzmin, N. K. Potkina *et al*., *BioNanoScience*, **10**, 486 (2020), https://doi.org/10.1007/s12668-020-00727-z
[65] A. R. Abd El-Aziz, A. Gurusamy, M. R. Alothman, S. M. Shehata, S. M. Hisham *et al*., *Saudi J. Biol. Sci*., **28**, 1093 (2021), https://doi.org/10.1016/j.sjbs.2020.11.036